

Novel Fabrication of Disorderly Exfoliated Sodium Montmorillonite in a Styrene–Butadiene Rubber Matrix

Qingguo Wang,¹ Yuan Zhong,¹ Xiaohong Zhang,² Zhihai Song²

¹Key Laboratory of Rubber-Plastics of Ministry of Education, Qingdao University of Science and Technology, Qingdao 266042, China

²SINOPEC Beijing Research Institute of Chemical Industry, Beijing 100013, China

Correspondence to: Q. Wang (E-mail: qwang@qust.edu.cn)

ABSTRACT: Using industrial technologies, we prepared a sodium montmorillonite (Na-MMT) slurry and an irradiated styrene–butadiene rubber (SBR) latex, and then spray dried them to produce a novel, ultrafine fully vulcanized powder SBR (UFPSBR)/Na-MMT nanocompound powder in which the nanoscale UFPSBR particles and exfoliated Na-MMT were isolated and stuck together. When the UFPSBR/Na-MMT nanocompound powder was mixed with crude SBR, the exfoliated Na-MMT was disorderly dispersed in the SBR matrix because of the carrier nature of the UFPSBR particle, which is compatible with SBR and disperses easily in the SBR matrix, and the SBR/UFPSBR/Na-MMT ternary nanocomposite was prepared. When compared with SBR/Na-MMT binary composites, the SBR/UFPSBR/Na-MMT ternary nanocomposite has a shorter vulcanization time, higher strength, and better flame retardancy because of the good dispersion of exfoliated Na-MMT in the SBR matrix with a Na-MMT loading range of 4 phr. © 2012 Wiley Periodicals, Inc. *J Appl Polym Sci* 000: 000–000, 2012

KEYWORDS: rubber; nanocomposites; dispersion; clay

Received 3 January 2011; accepted 21 March 2012; published online

DOI: 10.1002/app.37761

INTRODUCTION

In the past two decades, polymer/clay nanocomposites have attracted interest for both academic research and industrial applications because of their improved barrier properties, better flame retardancy, and higher strength.^{1–4} Generally, the exfoliated clay morphology in polymer/clay nanocomposites is recognized as superior because it exhibits better performance with lower clay loadings.^{5,6} However, the pristine clay is hydrophilic and easily aggregated in polymer matrix, and thus, it is difficult to get the exfoliated clay morphology in polymer/clay nanocomposites directly with pristine clay. Therefore, organic reagent-treated clay (organoclay) is widely utilized to prepare the polymer/clay nanocomposites because the organoclay is compatible with polymers and disperses well in a polymer matrix.^{5–9} For instance, the hydrophilic clay was previously organomodified with onium salts to promote a stable dispersion of clay layers in rubber/clay composites.^{10–13} Some polymer/clay nanocomposites have been developed by *in situ* polymerization intercalation, solution intercalation, and melt intercalation in the presence of organoclay. Unfortunately, a higher volume fraction of organoclay adversely affects the thermal stability of polymer nanocom-

posites.⁹ Additionally, the fabrication of organoclay is complex and costly and thus unacceptable to the polymer/clay nanocomposites industry. Therefore, the question of how to fabricate the polymer/clay nanocomposites directly with the pristine clay is a challenging one for the polymer/clay composite industry, including research and its applications.

In our previous research, we fabricated the ultrafine fully vulcanized powder rubber (UFPR) particles using the irradiation of rubber latex and spray drying. The SBR macromolecules of SBR latex were radical and vulcanized during irradiation process, leading to special crosslink structure of the irradiated rubber particles, higher crosslink density of SBR macromolecules outside due to the existence of trimethylol propane triacrylate (TMPTA) and lower crosslink density inside,¹⁴ and the UFPR particles were well dispersed in polymer matrix and improved some properties of polymer/UFPR composites.^{15–20} In the current study, using the industrial technologies of the preparation of exfoliated sodium montmorillonite (Na-MMT) slurry, rubber latex irradiation, and spray drying, we fabricated a novel ultrafine fully vulcanized powder styrene–butadiene rubber (UFPSBR)/Na-MMT nanocompound powder in which the

© 2012 Wiley Periodicals, Inc.

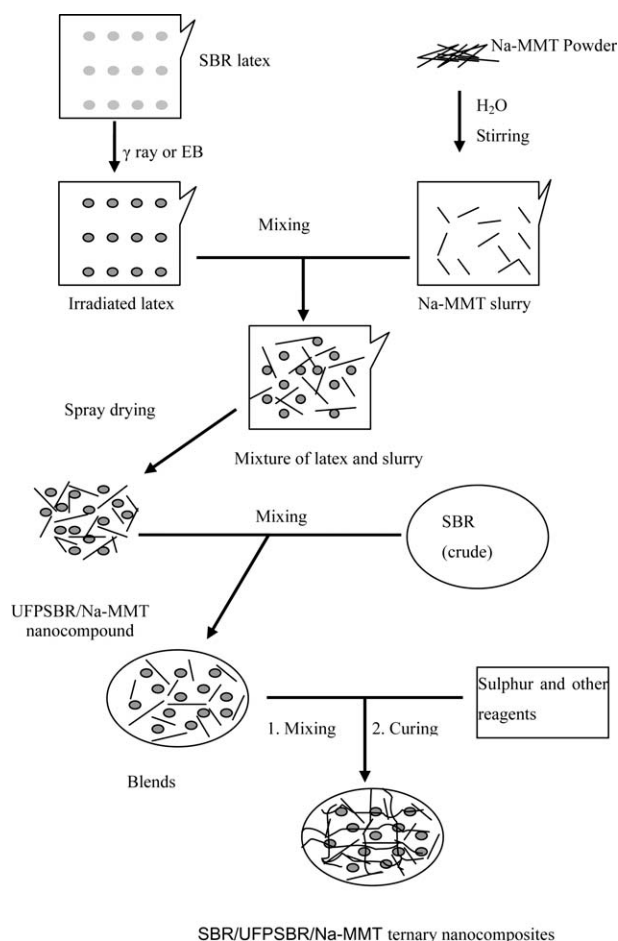


Figure 1. Fabrication schematic of SBR/UFPSBR/Na-MMT ternary nanocomposites.

nanoscale UFPSBR particles and exfoliated Na-MMT are isolated and stuck together. During the mixing of the UFPSBR/Na-MMT nanocomponent powder with crude SBR, the UFPSBR particles are easily dispersed in the SBR matrix because of their compatibility and special crosslink structure. Accordingly, the nanoscale-exfoliated Na-MMT was well dispersed in the SBR matrix because of the carrier nature of the UFPSBR particles, resulting in the fabrication of the SBR/UFPSBR/Na-MMT ternary nanocomposites adaptable to industry standards.²¹ The current study reports the dispersion of Na-MMT in the SBR matrix and its effects on specific properties of the SBR/UFPSBR/Na-MMT ternary nanocomposites.

EXPERIMENTAL

Materials

SBR (1502; styrene content: 23.5%) and SBR latex (DB50; styrene content: 50%) were purchased from SINOPEC Qilu Rubber Company of China. Na-MMT powder was supplied by Qinghe Chemistry Company of Hebei Province, China. TMPTA (irradiation sensitive) was purchased from Beijing Dongfang Chemical Company of China. Zinc oxide (99.7% purity) was prepared by Zhucheng Xiangtai Zinc Oxide Company of China. Sulfur (99.9% purity) was supplied by Gaomi Super Rubber Company of China.

CZ, a vulcanizing accelerate reagent (N-Cyclohexyl-2-benzothiazole sulfenamide), was fabricated by Zhaoyuan Rubber Reagent Company of China. Stearic acid (Hst) was prepared by Gaomi Youqiang Rubber Reagent Company of China.

Preparation of the SBR/UFPSBR/Na-MMT Ternary Nanocomposites

Figure 1 illustrates the fabrication procedure of the SBR/UFPSBR/Na-MMT ternary nanocomposites. First, five parts per hundred of rubber (phr) TMPTA was added dropwise into the SBR latex while stirring. After stirring for 1 h, the SBR latex was irradiated with 15 kGy under a 60 cobalt source or electron beam. The irradiated SBR latex and Na-MMT slurry (5 wt %) were well mixed into the slurry, in which the weight ratio of solid SBR to solid Na-MMT was 4 : 1. After spray drying, the fabrication of the UFPSBR/Na-MMT nanocomponent powder was complete. Second, the two rolls of a two-roller were adjusted to the adaptive distance at which bulk SBR becomes fluid at 60°C, and the 10 phr UFPSBR/Na-MMT nanocomponent powder was added into the 100 phr crude SBR. Finally, 5 phr ZnO, 1.0 phr CZ, 1.0 phr Hst, and 1.5 phr sulfur were added into the above-mentioned SBR compound, one after the other. Three minutes later, the SBR compound was sliced into 1.5- to 2-mm pieces by the two-roller. The SBR compound was vulcanized on a platen presser using 25 tons of pressure at a temperature of 150°C, and then the vulcanized SBR/UFPSBR/Na-MMT ternary nanocomposites were prepared.

As mentioned above, using the same UFPSBR/Na-MMT (wt/wt = 4/1) nanocomponent powder, we also prepared some other SBR/UFPSBR/Na-MMT ternary composites that contain 1, 3, 4, 5, and 10 phr Na-MMT, respectively. To study the effect of the UFPSBR/Na-MMT nanocomponent powder on specific properties of the SBR/UFPSBR/Na-MMT ternary composites, we prepared and studied some SBR/Na-MMT binary composites that contain 2, 4, 8, and 10 phr Na-MMT, respectively.

Measurements

Cure time (T_{c90}) values of neat SBR and various SBR composites were characterized using an oscillating disc rheometer (EK-2000) manufactured by Taiwan Gotech Testing Machine at 150°C.

X-ray diffraction (XRD) patterns of specimens were collected on a D/max 2500 VB2+/PC X-ray diffractometer with Cu K α radiation ($\lambda = 0.1514$ nm) from 1° to 10° with a scanning speed of 1°/min.

Crosslink density of the UFPSBR particles were characterized by the magnetic resonance crosslink density spectrometer (MRCDS 3500-D) in the magnetic field of 3.5 A/m with the frequency of 15 Hz at 70°C.

The micromorphology of the SBR/UFPSBR/Na-MMT ternary composites was observed with a transmission electron microscope (TEM; Philips Tecnai 20). The ultrathin sections for TEM image observation, approximately 50–100 nm thick, were microtomed at -80°C .

An EKT-2002GF servohydraulic test machine, produced by Taiwan Yezhong, was used for dynamic compression testing according to GB/T1687-1993. Cylindrical rubber specimens, 25

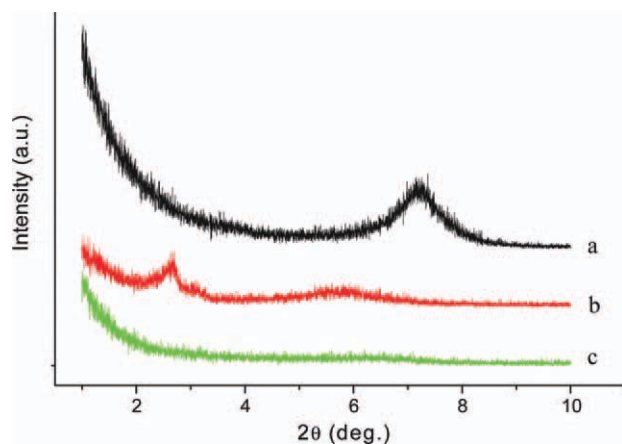


Figure 2. XRD patterns of (a) neat Na-MMT powder, (b) UFPSBR/Na-MMT (4/1, wt/wt) nanocompound powder, and (c) SBR/UFPSBR/Na-MMT (100/8/2, wt/wt/wt) ternary nanocomposites. [Color figure can be viewed in the online issue, which is available at wileyonlinelibrary.com.]

mm in height and 17.8 mm in diameter, were subjected to repeated compression. The frequency of loading was 30 Hz, and the static compressive load applied to specimens was 1 MPa. The test procedure was performed at 55°C for 25 min under constant load.

A cone calorimeter (standard; Fire Technology Testing) was used to evaluate the heat release rate (HRR) values of SBR specimens in the fire. The cone calorimeter was standardized according to ASTM E-1354 (2002) and ISO 5660. These SBR specimens with dimensions of $100 \times 100 \times 2 \text{ mm}^3$ were wrapped in aluminum dishes, and the up surface was exposed to a defined heat flux of 50 kW/m^2 .

Tensile test and tear strength of SBR specimens were performed according to GB/T528-1998 and GB/T529-1999, respectively. The speed of tensile and tear tests was 500 mm/min at room temperature.

RESULTS AND DISCUSSION

Dispersion of Exfoliated Na-MMT in SBR/UFPSBR/Na-MMT Ternary Composites

Figure 2 illustrates the XRD patterns of neat Na-MMT powder, UFPSBR/Na-MMT nanocompound powder, and the SBR/UFPSBR/Na-MMT ternary nanocomposites. In Figure 2 (peak a), the XRD pattern of neat Na-MMT powder exhibits an apparent diffraction peak at 7.21° (2θ) corresponding to the interlayer space of montmorillonite (d_{001}) of about 1.23 nm. In Figure 2 (peak b), there exist a higher diffraction peak at 2.67° and a slightly lower diffraction peak at 5.82° in the XRD patterns of UFPSBR/Na-MMT nanocompound powder, corresponding to the d_{100} values of 3.32 and 1.52 nm, respectively, which indicates that the Na-MMT layers are largely expanded in the UFPSBR/Na-MMT nanocompound powder. Figure 2 (peak c) shows the XRD pattern of the SBR/UFPSBR/Na-MMT ternary nanocomposites; no diffraction peak occurs in the 2θ range from 1° to 10° , which suggests that the Na-MMT in the SBR/UFPSBR/Na-MMT ternary nanocomposites exists in an exfoliated state.

It is well known that the interlayer space of Na-MMT is easily expanded largely due to hydrogen bonding in the Na-MMT slurry.^{4,22,23} After acute stirring, the enlarged interlayer space expanded, and the majority of Na-MMT platelets were separated in water and then the disorderly exfoliated Na-MMT platelets were obtained. After mixing with the irradiated SBR latex and spray drying, the disorderly exfoliated Na-MMT platelets were partitioned by UFPSBR particles in the UFPSBR/Na-MMT nanocompound powder. However, the small amount of Na-MMT whose interlayer space had not expanded sufficiently during the Na-MMT slurry fabrication and spray drying process led to small d_{100} values of Na-MMT, for instance, the d_{100} value of 1.52 nm. During the mixing process of the UFPSBR/Na-MMT nanocompound powder with crude SBR, the UFPSBR particles with the crosslink density of $1.826 \text{ E-4 mol/cm}^3$ were well dispersed in the SBR matrix because of their good flowability and good compatibility between UFPSBR particles and SBR matrix. Then the exfoliated Na-MMT platelets were also well dispersed in the SBR matrix because of the carrier nature of UFPSBR particles (the UFPSBR particles and exfoliated Na-MMT were isolated and stuck together). Therefore, there are no diffraction peaks in the XRD patterns of the SBR/UFPSBR/Na-MMT ternary nanocomposites in the 2θ range from 1° to 10° .

Figure 3 shows the TEM images of SBR/UFPSBR/Na-MMT ternary nanocomposites. The exfoliated Na-MMT is disorderly dispersed in the SBR matrix because of the carrier nature of the UFPSBR particles during the mixing of the UFPSBR/Na-MMT nanocompound powder with crude SBR, which coincides with the XRD patterns of the exfoliated Na-MMT in the SBR/UFPSBR/Na-MMT ternary nanocomposites.

Effects of the UFPSBR/Na-MMT Nanocompound Powder on the Vulcanizing Time of SBR/UFPSBR/Na-MMT Ternary Composites

The vulcanizing time (T_{c90}) is an important parameter for characterizing the vulcanizing degree of rubber macromolecules at a certain temperature. When the T_{c90} value is higher, the more energy is exhausted during rubber vulcanizing. As seen in Figure 4, as the UFPSBR/Na-MMT loading level increased, the T_{c90} values of the SBR/UFPSBR/Na-MMT ternary composites decreased, whereas the T_{c90} values of the SBR/Na-MMT binary composites decreased to an even lower value and then increased. As discussed in the above section, the 2 phr Na-MMT is dispersed in an exfoliated state in the SBR/UFPSBR/Na-MMT ternary composites. Therefore, a good dispersion of both UFPSBR particles and exfoliated Na-MMT platelets in the SBR matrix support a better dispersion of sulfur, ZnO, and CZ in the same matrix during the mixing process. These vulcanizing reagents then effectively perform in the vulcanizing reaction, leading to a lower T_{c90} value of SBR/UFPSBR/Na-MMT ternary nanocomposites, which explains why SBR/Na-MMT binary composites containing the same Na-MMT loading level have a higher T_{c90} value.

When the Na-MMT loading level increased to 4 phr, there were more aggregated Na-MMT particles in SBR/Na-MMT binary composites, which led to a worse dispersion of the vulcanization reagents and a higher T_{c90} value. In contrast, 4 phr exfoliated

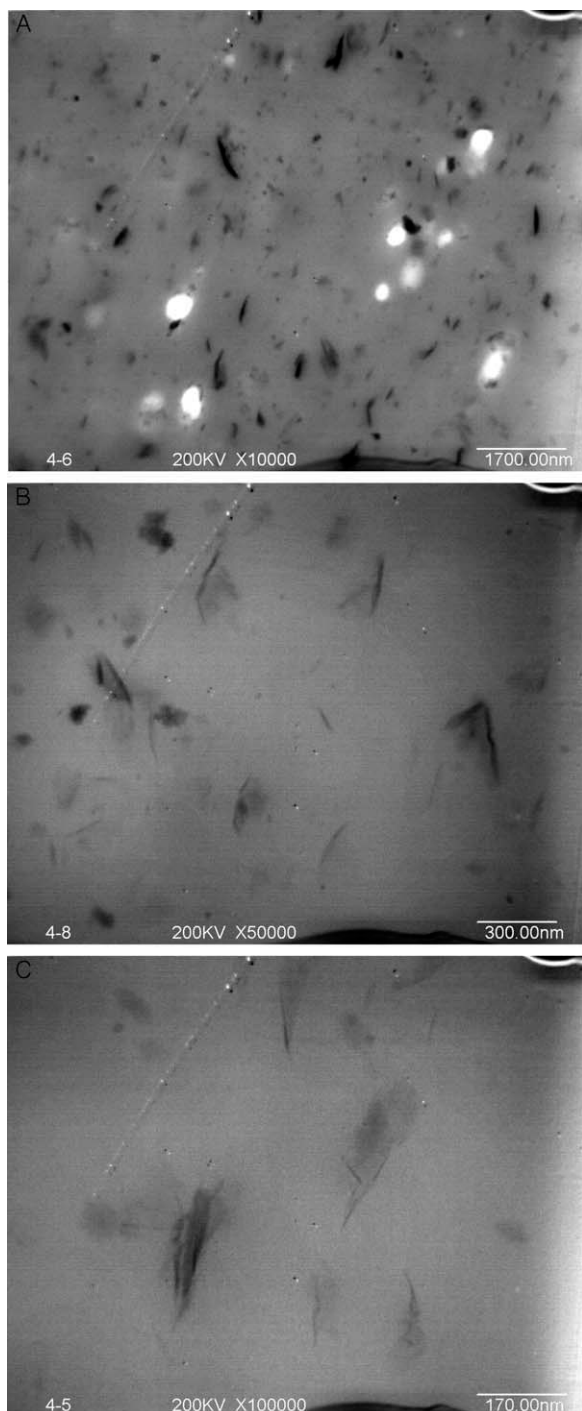


Figure 3. TEM images of the SBR/UFPSBR/Na-MMT (100/8/2, wt/wt/wt) ternary nanocomposites with different magnifications. A: $\times 10,000$; B: $\times 50,000$; C: $\times 100,000$. The black film in TEM images are the exfoliated Na-MMT layers.

Na-MMT in the UFPSBR/Na-MMT nanocompound powder had a good dispersion in the SBR matrix, which also enabled a better dispersion of the vulcanizing reagents and led to a lower Tc90 value of the SBR/UFPSBR/Na-MMT ternary composites. For the same reason, as the Na-MMT loading increased, the Na-MMT in the SBR/Na-MMT binary was easily aggregated in the SBR matrix, leading to higher Tc90 values, whereas the

Tc90 values of the SBR/UFPSBR/Na-MMT ternary composites containing the same exfoliated Na-MMT loadings decreased.

Mechanical Properties of SBR/UFPSBR/Na-MMT Ternary Composites

Figures 5 and 6 illustrate the curves of tensile strength, elongation at break, and tear strength versus Na-MMT loadings for both the SBR/UFPSBR/Na-MMT ternary composites and SBR/Na-MMT binary composites. With the increase in Na-MMT loading, the tensile strength and elongation at break of both the SBR/UFPSBR/Na-MMT ternary composites and the SBR/Na-MMT binary composites increased, indicating that both the UFPSBR/Na-MMT nanocompound powder and the Na-MMT powder exhibit the reinforcement effect. At the same Na-MMT loading level, when compared with SBR/Na-MMT binary composites, the SBR/UFPSBR/Na-MMT ternary composites displayed higher tensile strength. Meanwhile, the elongation at break of the SBR/UFPSBR/Na-MMT ternary composites increased to a high level at the 4 phr Na-MMT loading level, then increased slowly, and the tear strength of the SBR/UFPSBR/Na-MMT ternary composites increased to the highest level at the 4 phr Na-MMT loading level, then decreased to less than that of the SBR/Na-MMT binary composites in the Na-MMT loading range from 5 to 10 phr.

It is well known that the Na-MMT is easily aggregated into big particles in rubber matrix when it is mixed with crude SBR directly, and there is a small interface between the SBR matrix and Na-MMT particles in the SBR/Na-MMT binary composites. In contrast, the 2 phr exfoliated Na-MMT layers are well dispersed in SBR/UFPSBR/Na-MMT ternary composites, and there are larger interfaces and stronger interfacial interactions between the SBR matrix and the exfoliated Na-MMT layers in the SBR/UFPSBR/Na-MMT ternary composites, making it feasible that the exfoliated Na-MMT plays an important role in the reinforcement of the SBR/UFPSBR/Na-MMT ternary nanocomposites. On one hand, the exfoliated Na-MMT layers, wrapped with SBR macromolecules, acted as the physical crosslinks in

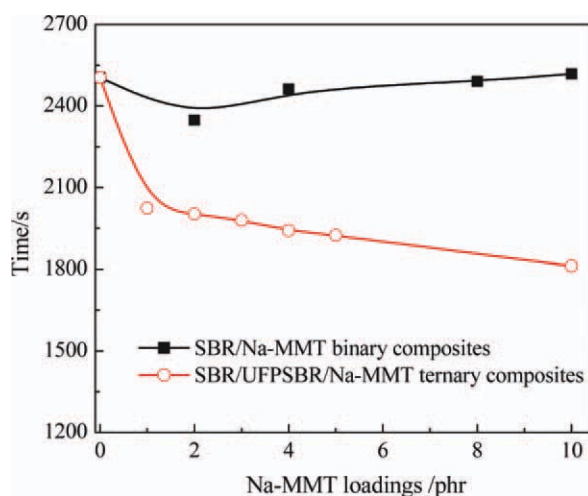


Figure 4. Influence of Na-MMT loadings on the vulcanizing time of various SBR composites. [Color figure can be viewed in the online issue, which is available at wileyonlinelibrary.com.]

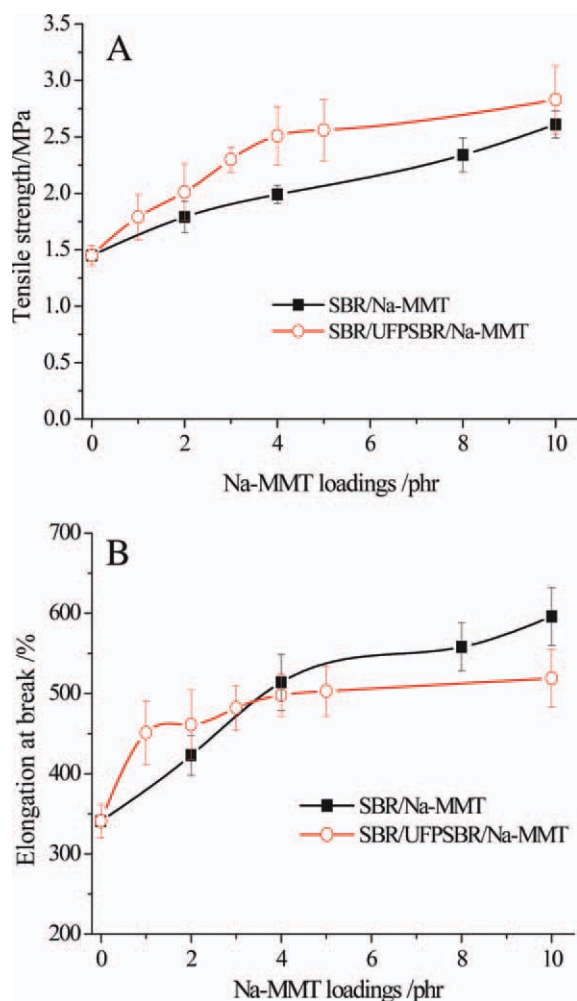


Figure 5. (A) Tensile strength and (B) elongation at break versus Na-MMT loading curves of both SBR/Na-MMT binary composites and SBR/UFPSBR/Na-MMT ternary composites. [Color figure can be viewed in the online issue, which is available at wileyonlinelibrary.com.]

SBR composites. On the other hand, a good dispersion of the UFPSBR particles and exfoliated Na-MMT layers also support the vulcanization of the SBR macromolecules, resulting in more chemical crosslinks in the SBR matrix. Therefore, it is easy to understand why the SBR/UFPSBR/Na-MMT ternary composites have higher tensile and tear strength when compared with the SBR/Na-MMT binary composites in the Na-MMT loading range of 4 phr because of the good dispersion of the nanoscale UFPSBR particles and exfoliated Na-MMT.

At the same 10 phr Na-MMT loading level, the SBR/UFPSBR/Na-MMT ternary composites have lower elongation at break and lower tear strength when compared with the SBR/Na-MMT binary composites, whereas the dominant tensile strength differences between these two SBR composites became smaller. When compared with the 10 phr Na-MMT in the SBR/Na-MMT binary composites, the 40 phr UFPSBR particles and the 10 phr Na-MMT in SBR/UFPSBR/Na-MMT ternary composites reduced the volume fraction of SBR matrix, and thus, the fraction of chemical crosslinks decreased; this finding may be the

major reason why the elongation at break and tear strength of the SBR/UFPSBR/Na-MMT ternary composites were smaller than that of the SBR/Na-MMT binary composites. On the other hand, too many filler particles in the SBR matrix also induced more physical crosslinks, which supports the reinforcement of both the SBR/UFPSBR/Na-MMT ternary composites and the SBR/Na-MMT binary composites. In addition, there are further explanations for the above results; however, in this study, we are not clear about the reinforcement mechanism of Na-MMT in the SBR composites.

Dynamic Compression Properties of SBR/UFPSBR/Na-MMT Ternary Nanocomposites

Table I lists some permanent set and heat build-up (ΔT) data of various SBR composite specimens. In this study, the neat SBR specimens were fractured during dynamic compression testing because of their low strength and there were no experimental data in Table I. As the Na-MMT loading increased, the permanent set values of SBR/Na-MMT binary composites decreased from 4.0 to 3.5 %, whereas their heat build-up increased from 7.2 to 9.1°C in the Na-MMT loading range of 2–10 phr. Meanwhile, the permanent set of the SBR/UFPSBR/Na-MMT ternary composites decreased from 2.5 to 2.1%, then increased to 8.3%, and the heat build-up values increased from 6.0 to 14.7°C in the Na-MMT loading range of 2–10 phr.

When compared with the SBR/Na-MMT binary composites, the SBR/UFPSBR/Na-MMT ternary composites with the same 2 phr Na-MMT loading level had lower permanent set and heat build-up values. As mentioned above (Figure 3), the 2 phr exfoliated Na-MMT and 8 phr UFPSBR particles were well dispersed in the SBR matrix, which supports the chemical crosslinks among the SBR macromolecules and explains the reason why the SBR/UFPSBR/Na-MMT ternary nanocomposites have better elasticity and lower permanent set than the SBR/Na-MMT binary composites during dynamic compression testing at the low Na-MMT loading level. It is well known that the aggregated Na-MMT particles display a higher stiffness than the rubber

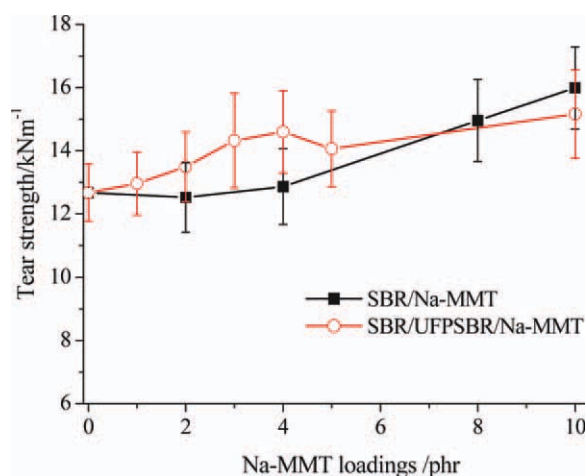


Figure 6. Tear strength versus Na-MMT loading curves of both SBR/Na-MMT binary composites and SBR/UFPSBR/Na-MMT ternary composites. [Color figure can be viewed in the online issue, which is available at wileyonlinelibrary.com.]

Table I. Permanent Set and Heat Build-Up Data of Various SBR Composites

	Neat SBR	SBR/Na-MMT binary composites (Na-MMT) (phr)			SBR/UFPSBR/Na-MMT ternary composites [UFPSBR/Na-MMT (phr/phr)]		
		2	4	10	8/2	16/4	40/10
Permanent set (%)	-	4.0	3.9	3.5	2.5	2.1	8.3
Heat build-up (ΔT , °C)	-	7.2	7.7	9.1	6.0	7.8	14.7

phase, and therefore, the heat build-up value generated among the aggregated Na-MMT particles is higher than those generated between the exfoliated Na-MMT layers and the rubber phase during dynamic compression testing. As a result, we infer that a good dispersion of the Na-MMT particles in the SBR matrix supports a low heat build-up value during dynamic compression testing.

However, at the same 10 phr Na-MMT loading level, the SBR/UFPSBR/Na-MMT ternary composites containing 10 phr Na-MMT and 40 phr UFPSBR particles have higher permanent set and heat build-up values than the SBR/Na-MMT binary composites. On one hand, too many UFPR particles and Na-MMT platelets in the SBR matrix are prone to aggregating, which induces worse chemical crosslinking of the SBR macromolecules and leads to a higher permanent set value for the SBR/UFPSBR/Na-MMT ternary composites. On the other hand, the friction probability among the aggregated 10 phr Na-MMT and aggregated 40 phr UFPSBR particles in the SBR/UFPSBR/Na-MMT ternary composites is higher than among the aggregated 10 phr Na-MMT particles in the SBR/Na-MMT binary composites during dynamic compression testing, thus leading to a higher heat build-up value of SBR/UFPSBR/Na-MMT ternary composites.

Effects of the UFPSBR/Na-MMT Nanocompound Powder on the Flame Retardancy of SBR Composites

Figure 7 illustrates the HRR curves of neat SBR, SBR/Na-MMT binary composites, and SBR/UFPSBR/Na-MMT ternary nanocomposites under a heat flux of 50 kW/m². When compared with neat SBR and SBR/Na-MMT binary composites, the SBR/

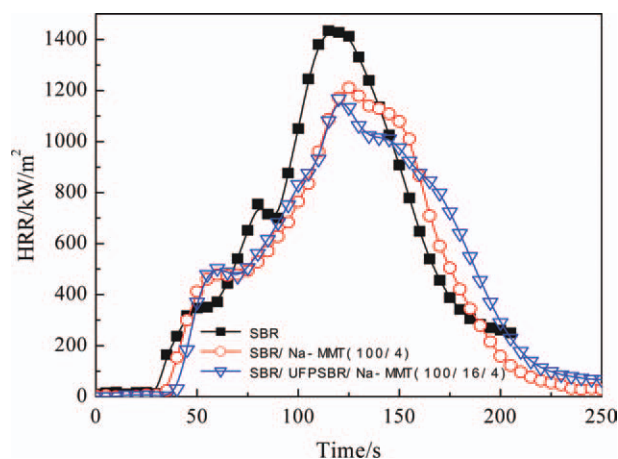


Figure 7. Heat release rate versus time of various SBR composites. [Color figure can be viewed in the online issue, which is available at [wileyonlinelibrary.com](http://www.wileyonlinelibrary.com).]

UFPSBR/Na-MMT ternary nanocomposites have a lower peak of HRR, and the average HRR value is also lower. Of note, the ignition time of the SBR/UFPSBR/Na-MMT ternary composites is 8 and 4 s longer than the neat SBR and SBR/Na-MMT binary composites, respectively. The above results show that both the UFPSBR/Na-MMT nanocompound and Na-MMT have good effect on the flame retardancy of SBR composites and that the SBR/UFPSBR/Na-MMT ternary nanocomposites have better flame retardancy. Under strong heat flux, combustible volatiles are released owing to the pyrolysis of the SBR macromolecule. As for the SBR/UFPSBR/Na-MMT ternary nanocomposites, a good dispersion of nanoscale Na-MMT layers has a better barrier effect on preventing the heat and O₂ of air from penetrating into the SBR macromolecule while preventing the combustible volatiles from transferring into the air, resulting in good flame retardancy of the SBR/UFPSBR/Na-MMT ternary nanocomposites. In contrast, the aggregated Na-MMT particles in the SBR/Na-MMT binary composites do not have the same flame-retardancy effect as the exfoliated Na-MMT layer in the SBR/UFPSBR/Na-MMT ternary composites.

CONCLUSIONS

For this study, we prepared a novel UFPSBR/Na-MMT nanocompound powder using industrial technologies to prepare a Na-MMT slurry and irradiation of SBR latex, to mix irradiated rubber latex and Na-MMT slurry, and to perform the spray drying. During the mixing of the UFPSBR/Na-MMT nanocompound powder with crude SBR, the exfoliated Na-MMT platelets in UFPSBR/Na-MMT nanocompound powder can be disorderly dispersed in the SBR matrix with the carrier support of the UFPSBR because the UFPSBR particles and the exfoliated Na-MMT are isolated and adhered to each other in the UFPSBR/Na-MMT nanocompound powder. Thus, we fabricated the SBR/UFPSBR/Na-MMT ternary nanocomposites. In the Na-MMT loading range of 4 phr, when compared with the SBR/Na-MMT binary composites, the SBR/UFPSBR/Na-MMT ternary nanocomposites containing the same Na-MMT loading level exhibit a shorter vulcanization time, higher strength, lower permanent set and heat build-up values, and higher flame retardancy because of the exfoliated Na-MMT layers in SBR matrix. However, at the same 10 phr Na-MMT loading level, too many UFPSBR particles and aggregated Na-MMT particles in the SBR/UFPSBR/Na-MMT ternary nanocomposite led to higher permanent set and heat build-up values than the SBR/Na-MMT binary composites because of the increased friction among fillers and the worsening chemical crosslinks of the SBR macromolecules.

ACKNOWLEDGMENTS

This research is supported by the National Natural Science Foundation of China (Grant No. 50873049), Shandong Young Scientists Encouragement Foundation (Grant No. 2007BS04038), and Scientific Research Foundation of Shandong Education Department (Grant No. J07YA12).

REFERENCES

1. Usuki, A.; Kawasumi, M.; Kojima, Y.; Fukushima, Y.; Okada, A.; Kurauchi, T.; Kamigaito, O. *J. Mater. Res.* **1993**, *8*, 1179.
2. Ratna, D.; Simon, G. P. *J. Polym. Mater.* **2002**, *19*, 143.
3. Wang, M. S.; Pinnavaia, T. J. *Chem. Mater.* **1994**, *6*, 468.
4. Yui, T.; Yoshida, H.; Tachibana, H.; Tryk, D. A.; Inoue, H. *Langmuir* **2002**, *18*, 891.
5. Ma, J.; Yu, Z.-Z.; Kuan, H.-C.; Dasari, A.; Mai, Y.-W. *Macromol. Rapid Commun.* **2005**, *26*, 830.
6. Li, Y.; Shimizu, H. *Polymer* **2004**, *45*, 7381.
7. Wan, C. Y.; Qiao, X. Y.; Zhang, Y.; Zhang, Y. X. *J. Appl. Polym. Sci.* **2003**, *89*, 2184.
8. You, C. J.; Jia, D. M.; Zhen, Z. Y.; Ding, K.; Xi, S.; Mo, H. L.; Zhang, Y. H. *Chinese J. Polym. Sci.* **2003**, *21*, 551.
9. Xie, W.; Gao, Z.; Pan, W.-P.; Hunter, D.; Singh, A.; Vaia, R. *Chem. Mater.* **2001**, *13*, 2979.
10. Kaneko, M.L. Q.A.; Romero, R. B.; do Carmo Gonçalves, M.; Yoshida, I. V. P. *Eur. Polym. J.* **2010**, *46*, 881.
11. Mathew, G.; Rhee, J. M.; Lee, Y.-S.; Park, D. H.; Nah, C. *J. Ind. Eng. Chem.* **2008**, *14*, 60.
12. Balakrishnan, S.; Start, P. R.; Raghavan, D.; Hudson, S. D. *Polymer* **2005**, *46*, 11255.
13. Gatos, K. G.; Karger-Kocsis, J. *Polymer* **2005**, *46*, 3069.
14. Qiao, J. L.; Wei, G. S.; Zhang, X. H.; Zhang, S. J.; Gao, J. M.; Zhang, W.; Liu, Y. Q.; Li, J. Q.; Zhang, F. R.; Zhai, R. L.; Shao, J. B.; Yan, K. K.; Yin, H. *U.S. Pat.* 6,423,760 (**2002**).
15. Liu, Y.; Zhang, X.; Gao, J.; Huang, F.; Tan, B.; Wei, G.; Qiao, J. *Polymer* **2004**, *45*, 275.
16. Zhang, M.; Liu, Y.; Zhang, X.; Gao, J.; Huang, F.; Song, Z.; Wei, G.; Qiao, J. *Polymer* **2002**, *43*, 5133.
17. Zhang, X.; Liu, Y.; Gao, J.; Huang, F.; Song, Z.; Wei, G.; Qiao, J. *Polymer* **2004**, *45*, 6959.
18. Gui, H.; Zhang, X.; Liu, Y.; Dong, W.; Wang, Q.; Gao, J.; Song, Z.; Lai, J.; Qiao, J. *Compos. Sci. Technol.* **2007**, *67*, 974.
19. Ma, H.; Wei, G.; Liu, Y.; Zhang, X.; Gao, J.; Huang, F.; Tan, B.; Song Z.; Qiao J. *Polymer* **2005**, *46*, 10568.
20. Wang, Q.; Zhang, X.; Liu, S.; Gui, H.; Lai, J.; Liu, Y.; Gao, J.; Huang, F.; Song, Z.; Tan, B.; Qiao, J. *Polymer* **2005**, *46*, 10614.
21. Liu, Y. Q.; Qiao, J. L.; Zhang, X. H.; Huang, F.; Gao, J. M.; Tan, B. H.; Wei, G. S.; Song, Z. H.; Chen, Z. D. *Chinese Pat. CN03109108.3* (**2003**).
22. Strawhecker, K. E.; Manias, E. *Chem. Mater.* **2000**, *12*, 2943.
23. Kyung, K. Y.; Suk, C. Y.; Hyun, W. K.; Jae, C. I. *Chem. Mater.* **2002**, *14*, 4990.